



OPEN

Up-regulation of blood-circulating TIM-4-expressing monocytes and potential diagnostic biomarker sTIM-4 in primary liver cancer

Yifeng Yang^{1,8}, Yan Wei^{2,8}, Yilian Zhao^{3,8}, Chao Ye⁴, Dan Zeng⁵, Xiaoxing Zhou⁴, Mengru Xie³, Xingcai Chen¹, Jilin Qing⁶✉ & Zhizhong Chen⁷✉

Primary hepatocellular carcinoma (PHC) remains a globally prevalent malignancy, where early diagnosis is critical. Monocytes have been implicated in tumor progression. This study investigated the expression of T cell immunoglobulin and mucin domain-containing protein 4 (TIM-4/TIMD4) in PHC tissues and peripheral blood monocytes, and assessed the clinical relevance of soluble TIM-4 (sTIM-4). Immunohistochemistry and bioinformatics analyses revealed reduced TIM-4 expression in PHC tissues, which correlated with immune cell infiltration. Flow cytometry showed elevated TIM-4 expression in circulating monocytes of PHC patients, predominantly within the intermediate subset (91.7%). sTIM-4 and monocyte TIM-4 levels were positively correlated with alpha-fetoprotein (AFP), alanine aminotransferase (ALT), aspartate aminotransferase (AST), gamma-glutamyl transferase (GGT), alkaline phosphatase (ALP), and negatively correlated with albumin (ALB). Notably, sTIM-4 levels were significantly higher in patients with a history of hepatitis. Logistic regression indicated that elevated sTIM-4 was associated with a 2.29-fold increased risk of PHC. ROC analysis demonstrated that the combination of sTIM-4 and AFP improved diagnostic accuracy for PHC. In conclusion, TIM-4 is downregulated in PHC tissues but upregulated in circulating intermediate monocytes, suggesting its dual role in tumor immunobiology. The combined measurement of sTIM-4 and AFP enhances diagnostic sensitivity and offers predictive value for PHC risk stratification.

Keywords Primary liver cancer, TIM-4, sTIM-4, Blood-circulating monocyte subsets

Liver cancer is among the most prevalent malignant tumors worldwide. In 2020, an estimated 90.6 million individuals were diagnosed with the disease^{1,2}, making it the third leading cause of cancer-related deaths globally, with a relative five-year survival rate of approximately 18%¹. The high incidence and mortality underscore its poor prognosis. Liver cancer can be classified into primary liver cancer (PHC)—characterized by aggressive biological behavior—and secondary liver cancer³. Hepatocellular carcinoma (HCC, also referred to as LIHC) accounts for 80–90% of PHC cases, while intrahepatic cholangiocarcinoma contributes to 10–15%⁴. Most PHC patients have underlying chronic liver conditions, commonly due to hepatitis B virus (HBV) or hepatitis C virus (HCV) infection, with HBV predominating in Asia⁵.

The slow pace of advancements in prevention and early detection has contributed to the rising incidence of PHC. Currently, the sensitivity of abdominal ultrasonography for early PHC detection remains suboptimal, especially in patients with obesity or non-viral liver disease⁶. While blood-based monitoring strategies show promise, they still require further validation before clinical practice⁶. In recent years, immune checkpoint inhibitor (ICI)-based therapies have become widely used for advanced PHC treatment⁷. Although ICIs,

¹Laboratory Department, People's Hospital of Guilin, Guilin 541000, China. ²Graduate College, Guangxi University of Chinese Medicine, Nanning 530200, China. ³Department of Clinical Laboratory, The First Affiliated Hospital of Guangxi Medical University, Key Laboratory of Clinical Laboratory Medicine of Guangxi Department of Education, Nanning 530021, China. ⁴Clinical Medical College, Guilin Medical University, Guilin 541000, China. ⁵Genetics and Precision Medicine Laboratory, Affiliated Hospital of Guilin Medical University, Guilin 541000, China. ⁶Reproductive Medicine Center, People's Hospital of Guangxi Zhuang Autonomous Region, Nanning 530000, China. ⁷Joint Inspection Center of Precision Medicine, People's Hospital of Guangxi Zhuang Autonomous Region, Nanning 530000, China. ⁸Yifeng Yang, Yan Wei and Yilian Zhao contributed equally to this work. ✉email: heroandgirl@163.com; tjchenzz@126.com

especially in combination with other agents, have improved survival outcomes for some patients, sustained benefits remain limited in late-stage disease. As a result, identifying novel molecular targets associated with liver cancer has become a major focus in PHC research and treatment.

The human T-cell immunoglobulin and mucin domain-containing (TIM) gene family was first identified by McIntire's team in 2001 during studies on asthma susceptibility⁸. This family includes three human TIM genes—TIM-1, TIM-3, and TIM-4—which encode proteins involved in immune regulation^{9,10}. TIM-1 and TIM-3 are predominantly expressed on T cells and play roles in regulating apoptosis and immune tolerance¹¹. In contrast, TIM-4, also known as TIMD4, (TIMD4 for Mesh name, TIM-4 for commonly used name) is mainly expressed on antigen-presenting cells such as macrophages and dendritic cells (DCs). As a natural ligand of TIM-1 and a phosphatidylserine receptor, TIM-4 facilitates the phagocytosis of apoptotic cells by macrophages. It also modulates T-cell activation and tolerance, contributing to immune homeostasis¹². While the role of TIM-4 has been extensively investigated in malignancies such as cervical cancer, rectal cancer, and non-small cell lung cancer (NSCLC)¹³⁻¹⁵, its involvement in PHC remains poorly understood.

Recent studies have shown that TIM-4 is highly expressed in monocytes from patients with acute ischemic stroke, particularly within non-classical and intermediate monocyte subsets^{16,17}. Its expression was positively correlated with the National Institutes of Health Stroke Scale (NIHSS) score¹⁸. However, limited research exists on the regulatory function of TIM-4 in tumors, especially PHC. To date, no studies have reported the expression of TIM-4 in circulating monocytes or its concentration in plasma among PHC patients. In our bioinformatics analysis, we identified that TIM-4 exhibits reduced transcriptional and protein expression levels in liver cancer tissues. This pattern is distinct from the typical upregulation observed in many oncogenes and suggests that TIM-4 may have context-dependent biological functions. Notably, TIM-4 is highly expressed in other solid tumors, further highlighting its potential unique role in LIHC. Our analysis also revealed significant differential expression of TIMD4 in monocytes derived from LIHC patients. Monocytes and their related cell subsets play crucial regulatory roles in cancer development by influencing tumor growth, metastasis, and the tumor microenvironment¹⁹. Given the critical involvement of monocytes in these processes, we hypothesize that TIMD4 may be intricately linked to the function of monocytes during tumor progression in LIHC. This hypothesis forms the basis of our investigation and provides a strong rationale for focusing on the interplay between TIMD4 and monocytes in the context of LIHC.

Therefore, this study investigates TIM-4 expression in peripheral blood monocytes and plasma of PHC patients, alongside established PHC screening markers such as alpha-fetoprotein (AFP) and routine liver function indicators—including alanine aminotransferase (ALT), aspartate aminotransferase (AST), alkaline phosphatase (ALP), gamma-glutamyl transferase (GGT), total bilirubin (TBIL), albumin (ALB), prealbumin (PA), and albumin-to-globulin ratio (A/G). The aim is to explore TIM-4's diagnostic and therapeutic potential in PHC.

Materials and methods

Identification of TIM-4 (TIMD4) expression and clinical characteristics of PHC (LIHC)

TIMD4 expression data and comprehensive clinical records were obtained from The Cancer Genome Atlas (TCGA) database (<https://cancer.gov/tcga>). Expression levels of TIMD4 across various cancer types and its correlation with clinical characteristics in liver hepatocellular carcinoma (LIHC) were analyzed using online bioinformatics platforms including TIMER2.0, GEPIA, HPA, and UALCAN. The expression of TIMD4 in tumor tissues was further validated through immunohistochemical data from the HPA database.

Prognostic significance of TIMD4 in LIHC

The prognostic significance of TIMD4 in liver hepatocellular carcinoma was assessed using the Kaplan–Meier Plotter database. The TIMD4 gene identifier was selected, and the "automatic selection of the best cut-off" feature was employed.

In our bioinformatics analysis, to determine the optimal cutoff value for defining "high" and "low" TIM-4 expression groups, we performed receiver operating characteristic (ROC) curve analysis. This analysis involves plotting the relationship between the true positive rate (sensitivity) and the false positive rate (1- specificity) at various threshold settings. By calculating the area under the ROC curve (AUC), we quantified the overall diagnostic accuracy of our test. The optimal cutoff value was determined by identifying the point on the ROC curve that corresponds to the maximum AUC, representing the best balance between sensitivity and specificity. This ensures accurate differentiation between the groups while minimizing misclassifications.

Correlation genes with TIMD4 in LIHC

UALCAN utilizes TCGA gene expression data from normal and tumor tissues to illustrate the expression patterns of specific genes in liver hepatocellular carcinoma (LIHC). Gene expression values are transformed into Log2(TPM + 1) values, with a color-coded scale where blue indicates low expression and red indicates high expression. A legend is provided to explain the color coding. Genes with very low expression (Median TPM < 0.5) were excluded from the analysis. The heatmap includes genes with a Pearson correlation coefficient (Pearson-CC) exceeding 0.72 with TIMD4, highlighting a strong association with TIMD4 expression. This suggests potential functional or regulatory relationships between TIMD4 and these genes.

Immune infiltration analysis by TIMER2.0 and CIBERSORT

The association between TIMD4 expression and six types of tumor-infiltrating immune cells in LIHC was examined using the TIMER2.0 database. A scatter plot was generated to depict these relationships, providing insight into the potential immunomodulatory role of TIMD4 in LIHC.

CIBERSORT was utilized to quantify tumor-infiltrating immune cells using a deconvolution algorithm based on support vector regression, inferring cell proportions from gene expression profiles. A total of 424 LIHC patient samples were retrieved from the TCGA database. Patients were stratified into high and low TIMD4 expression groups. CIBERSORT was used to quantify 22 types of tumor-infiltrating immune cells in both groups. The analysis focused on differences in immune cell composition between the high and low TIMD4 expression groups, as well as the correlation between TIMD4 levels and immune cell infiltration.

General information collection

A total of 30 pairs pathological tissue sections from newly diagnosed PHC patients (2015–2022) at the People's Hospital of Guangxi Zhuang Autonomous Region (IEC approval No.:KY-KJT-2023-111) were analyzed. For each case, both cancerous and matched paracancerous tissues were examined. All 30 PHC cases were confirmed as hepatocellular carcinoma, comprising 24 males and 6 females, with 17 patients aged ≥ 50 years and 13 aged < 50 years. Of these, 21 had a history of hepatitis, and 9 did not. AFP levels were ≥ 400 ng/mL in 8 cases and < 400 ng/mL in 18 cases (4 cases missing data). Tumor size was ≥ 5 cm in 12 cases and < 5 cm in 15 cases (3 cases missing data). Twenty-four patients had a single tumor nodule, while 6 had multiple (≥ 2) nodules. Additionally, 23 non-PHC liver tissue samples were collected during the same period, including 19 hepatic cysts, 3 cases of nodular hyperplasia, and 1 case of bile duct stones with purulent cholecystitis.

Venous blood samples were collected from 29 newly diagnosed patients with primary hepatocellular carcinoma (PHC) at Guilin People's Hospital between May 2021 and January 2022 (IEC approval No.: 2020-046KY). Inclusion criteria were: newly diagnosed PHC with a definitive diagnosis, complete clinical data, and availability of relevant test results (AFP, TBIL, ALP, GGT, ALB, PA, and HBsAg). The cohort included 25 males and 4 females, with a median age of 58 years (IQR: 50.5–67.5). Patients with other malignancies were excluded. PHC diagnosis followed the Standards for the Diagnosis and Treatment of Primary Liver Cancer (2019 edition)²⁰. For the control group, healthy individuals undergoing routine physical examinations at Guilin People's Hospital during the same period were selected, comprising 24 males and 6 females with a median age of 57 years (IQR: 47.5–68.25).

All research protocols were reviewed and approved by the Ethics Committees/Institutional Review Boards of the People's Hospital of Guangxi Zhuang Autonomous Region and Guilin People's Hospital. Written informed consent was obtained from all participants, and the study was conducted in accordance with the Declaration of Helsinki.

Immunohistochemistry

Paraffin-embedded pathological tissue sections were processed using standard immunohistochemical procedures, including baking, dewaxing, antigen retrieval, quenching, blocking, and incubation with primary and secondary antibodies, followed by color development and mounting. In the histochemical experiments, we quantified the positively stained cells based on cytoplasmic color (light yellow, brown, or tan). Under high magnification, we randomly selected five fields from each pathological slide, counted 100 cells per field (totaling 500 cells), and calculated the percentage of positive cells and staining intensity for each slide. The staining range (percentage of positive cells) was scored as follows: 0% = 0, 1–25% = 1, 26–50% = 2, 51–75% = 3, 76–100% = 4. Staining intensity (color intensity) was scored as follows: no staining = 0, light yellow = 1, brown = 2, tan = 3. The immunoreactive score (IRS) was calculated as the product of the percentage value and the staining intensity score. Based on the IRS, samples were classified into low expression (IRS ≤ 4) and high expression (IRS > 4) groups.

Detection of blood-circulating monocyte subsets by flow cytometry

Peripheral blood mononuclear cells (PBMCs) were analyzed by flow cytometry. Classical, intermediate, and non-classical monocyte subsets were labeled using antibodies against CD14 (APC), CD16 (FITC), and TIM-4 (PE). TIM-4 expression was assessed in each monocyte subset. Control groups included blank and isotype controls.

ELISA to detect the expression level of sTIM-4

Soluble TIM-4 (sTIM-4) levels in peripheral blood plasma were measured using a commercially available TIMD4 ELISA kit.

Statistical analysis

Statistical analyses were conducted using R (v3.6.2), SPSS 26.0, and GraphPad Prism 8.0. Categorical variables were analyzed using the χ^2 test or Fisher's exact test. For normally distributed continuous data, the t-test was used. Correlations were assessed using Spearman's rank correlation. A p-value < 0.05 (two-tailed) was considered statistically significant.

Results

TIMD4 is weakly expressed in cancer tissues of LIHC

Using the TIMER2.0 and UALCAN databases, we observed dysregulation of TIMD4 at both the transcriptional and protein levels across various cancer types compared to normal tissues. Specifically, in liver hepatocellular carcinoma (LIHC), TIMD4 was significantly downregulated in tumor tissues relative to normal liver tissue ($P = 5.39 \times 10^{-20}$), as shown in Fig. 1A–D. This pattern was corroborated by pathological immunohistochemistry from the Human Protein Atlas (Fig. 1E,G). In addition, analysis via UALCAN revealed a marked reduction in TIMD4 promoter methylation in LIHC samples (Fig. 1E).

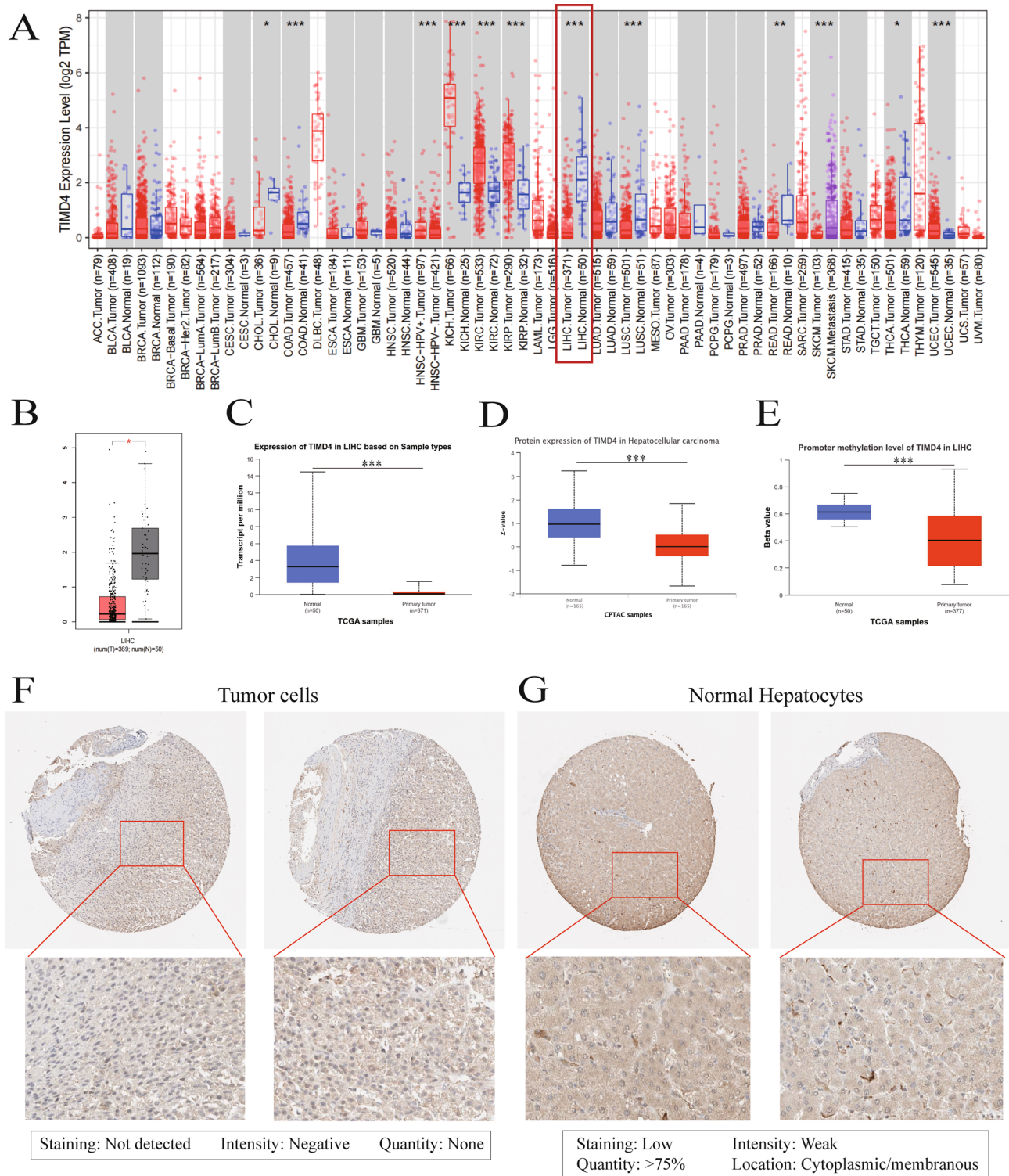


Fig. 1. Expression level of TIMD4 in LIHC. **(A)** Transcriptional expression level of TIMD4 in different cancers using TIMER2.0. **(B)** Transcriptional expression level of TIMD4 in LIHC by GEPIA. **(C)** Transcriptional expression level of TIMD4 in LIHC by UALCAN. **(D)** Protein expression of TIMD4 in LIHC by UALCAN. **(E)** Expression of TIMD4 methylation promoter gene in LIHC by UALCAN. **(F)** Pathological histochemistry of tumor tissues in LIHC (ID: CAB026027). **(G)** Pathological histochemistry of normal tissues in liver (ID: CAB026027). *P < 0.05, **P < 0.01, ***P < 0.001.

TIMD4 expression and clinical characteristics analysis

To elucidate TIMD4's role in LIHC progression, we conducted correlation analyses between its expression and clinical parameters using UALCAN (Fig. 2A–I). TIMD4 expression showed no significant association with gender, body weight, race, TP53 mutation status, or tumor grade. However, it was significantly correlated with patient age, lymph node metastasis, and tumor pathological subtype. Notably, TIMD4 expression was significantly lower in advanced tumor stages (stages 3 and 4, $P < 0.05$), suggesting a tumor-suppressive role during LIHC progression.

TIMD4 expression and overall survival (OS)

Kaplan–Meier survival analysis, based on data from 419 LIHC patients in public databases (<https://kmplot.com/analysis/>), revealed that higher TIMD4 expression is associated with improved prognosis and prolonged overall survival (OS; Fig. 2J).

Correlation genes with TIMD4

We further performed a gene co-expression analysis using UALCAN, identifying genes with expression profiles correlated with TIMD4 in LIHC (Fig. 2G). These findings were visualized to illustrate the relative expression of each gene within the cohort.

The heatmap clearly shows differential expression of TIMD4 and related genes between tumor and normal tissues. Genes such as TIMD4, LILRB5, and STEAP4 exhibit significantly lower expression levels in tumor tissues compared to normal tissues, as indicated by the color change from blue to red. In contrast, genes like RNASE1 and CTSK show higher expression levels in tumor tissues, with a color change from red to blue. Genes such as ATP8B4, POPDC2, and FOLR2 demonstrate minimal expression changes, evidenced by little color variation. This pattern suggests diverse regulatory mechanisms and functional roles of these genes in the context of liver cancer.

Correlation between TIMD4 expression level and the proportion of 22 immune cells

To investigate the immunological context, we employed CIBERSORT to estimate the relative abundance of 22 tumor-infiltrating immune cell types in LIHC samples stratified by high and low TIMD4 expression. The resulting histograms display the immune cell composition across the two groups (Fig. 3C). Notably, monocyte infiltration was significantly higher in the TIMD4 high-expression group compared to the low-expression group ($P < 0.05$). The optimal cutoff value for TIMD4 expression was determined using ROC curve analysis, ensuring the best trade-off between sensitivity and specificity. This algorithm determines the optimal cut-off value based on the maximum AUC, thus achieving the best trade-off between sensitivity and specificity for differentiating tumor from normal tissue.

The results of the analysis revealed differences in the proportion of immune cells in the TIMD4 low- and high-expression groups in LIHC samples. Among them, the infiltration of monocytes in the TIMD4 high-expression group was higher than that in the TIMD4 low-expression group, showing a significant difference ($P < 0.05$); the infiltration of M0 macrophages in the TIMD4 low-expression group was higher than that in the TIMD4 high-expression group, with a significant difference ($P < 0.001$; Fig. 3D).

The correlation between TIMD4 expression and immune cell infiltration in liver hepatocellular carcinoma (LIHC) was examined. TIMD4 expression showed a significant positive correlation with monocytes ($P < 0.001$), M2 macrophages ($P = 0.006$), and CD8⁺ T cells ($P = 0.03$). Conversely, it was negatively correlated with M0 macrophages ($P < 0.001$), regulatory T cells (Tregs; $P = 0.019$), resting mast cells ($P = 0.023$), and resting dendritic cells (DCs; $P = 0.031$) (Fig. 3E).

Pathological analysis

Immunohistochemical analysis revealed that TIM-4 was predominantly localized in the cytoplasm of hepatocytes and was detectable in cancerous tissues, adjacent non-tumorous tissues, and normal liver tissues (Fig. 4A). Among cancer tissues, 18 cases (60%) exhibited low TIM-4 expression and 12 cases (40%) showed high expression. In adjacent tissues, 9 cases (30%) had low expression while 21 cases (70%) had high expression. In non-cancerous liver tissues, low and high TIM-4 expression were observed in 5 cases (21.7%) and 18 cases (78.3%), respectively. The differences in TIM-4 expression between cancerous and non-cancerous tissues were statistically significant ($P < 0.05$; Fig. 4B). These findings indicate that TIM-4 expression is reduced in liver cancer tissues and may serve as a diagnostic marker for distinguishing malignant from benign hepatic lesions.

Chi-square analysis demonstrated that TIM-4 expression in PHC tissues was not significantly associated with patient age, sex, hepatitis B history, AFP levels, tumor number, tumor size, or other clinicopathological features.

Differences in the expression levels of blood-circulating monocyte subsets in PHC patients

No significant differences were found in sex distribution or age between the PHC and control groups ($P > 0.05$), thereby minimizing the confounding effects of these variables. Circulating monocytes were categorized into three subsets based on surface expression of CD14 (lipopolysaccharide receptor) and CD16 (Fc_Y receptor): classical (CD14⁺⁺CD16⁻), non-classical (CD14⁺CD16⁺⁺), and intermediate (CD14⁺⁺CD16⁺). The proportions of these subsets in PHC patients and healthy controls were evaluated using flow cytometry (Fig. 4C,D). The classical subset comprised 61% (IQR: 45.8–74.45) in PHC patients and 69.3% (IQR: 45.7–80.68) in controls, with no statistically significant difference ($P > 0.05$; Fig. 4E). Intermediate monocytes were significantly increased in the PHC group—8.3% (IQR: 4.8–11.85) versus 3.35% (IQR: 2.58–6.65) in controls ($P < 0.05$; Fig. 4F). No significant difference was observed in non-classical monocytes between PHC patients (14.3%; IQR: 6.65–24.45) and controls (19.35%; IQR: 8.63–31.45; $P > 0.05$; Fig. 4G).

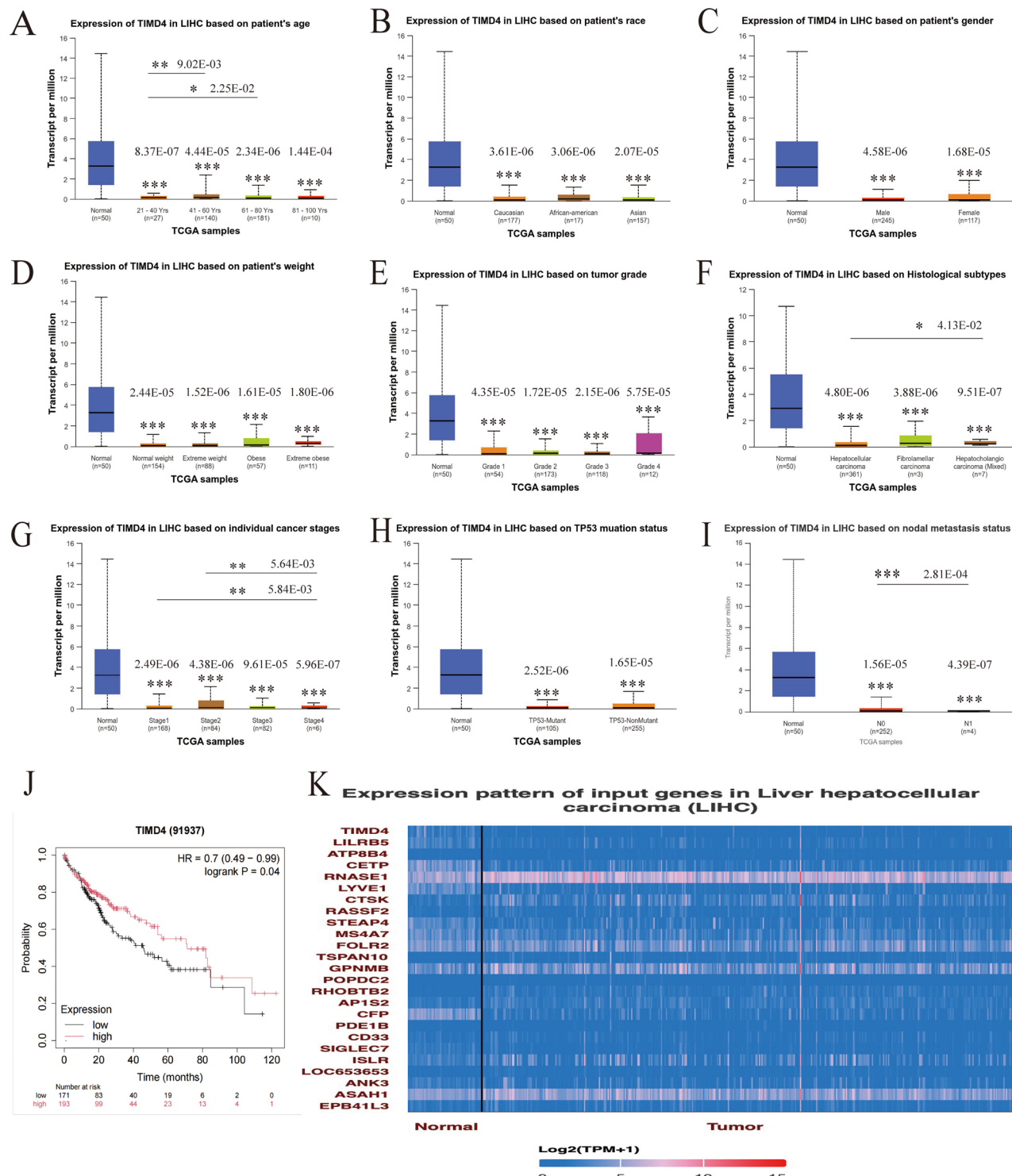


Fig. 2. Clinical characteristics of MLLT11 in LIHC (with p value). (A) Expression of TIMD4 in LIHC based on the patient's age. (B) Expression of TIMD4 in LIHC based on the patient's race. (C) Expression of TIMD4 in LIHC based on the patient's gender. (D) Expression of TIMD4 in LIHC based on the patient's weight. (E) Expression of TIMD4 in LIHC based on tumor grade. (F) Expression of TIMD4 in LIHC based on the patient's histological subtypes. (G) Expression of TIMD4 in LIHC based on individual cancer stage. (H) Expression of TIMD4 in LIHC based on TP53 mutation status. (I) Expression of TIMD4 in LIHC based on nodal metastasis status. (J) Prognostic significance of TIMD4 in LIHC. (K) Correlation genes with TIMD4. * $P < 0.05$, ** $P < 0.01$, *** $P < 0.001$.

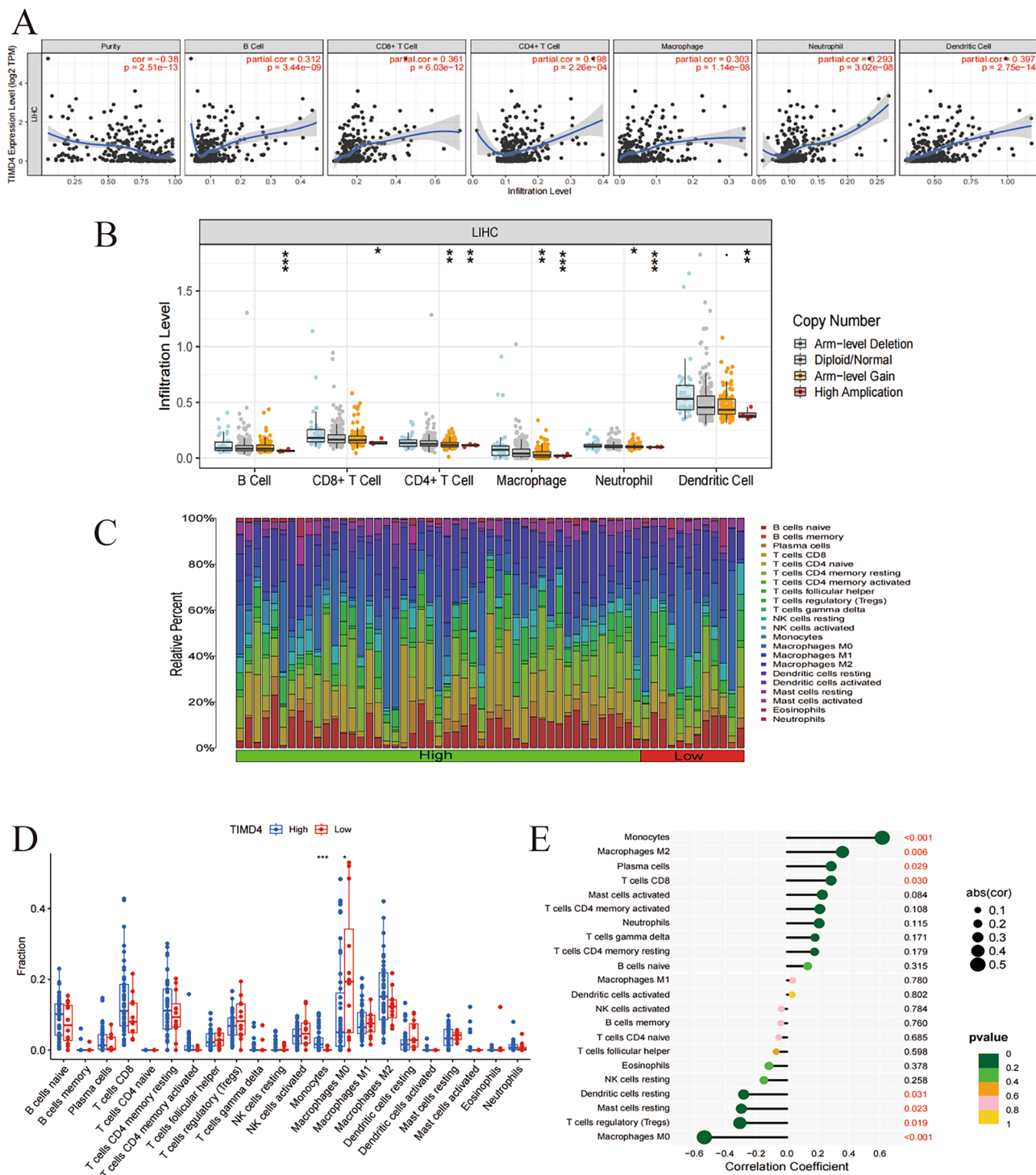


Fig. 3. Correlation between TIMD4 expression level and LIHC immune cell infiltration. (A) Scatter plot showing the correlation of six immune cell with TIMD4 expression in TIMER2.0. (B) Correlation of CNV of TIMD4 gene in somatic cells and the infiltration level of six immune cells in LIHC in TIMER2.0. (C) Relative percent of 22 immune cells between the low- and the high-expression groups of TIM-4 in LIHC by CIBERSORT. (D) Infiltration of immune cells in the TIMD4 low- and high-expression groups in LIHC samples by CIBERSORT. (E) Correlation between TIMD4 expression level and LIHC immune cell infiltration by CIBERSORT. * $P < 0.05$, ** $P < 0.01$, *** $P < 0.001$.

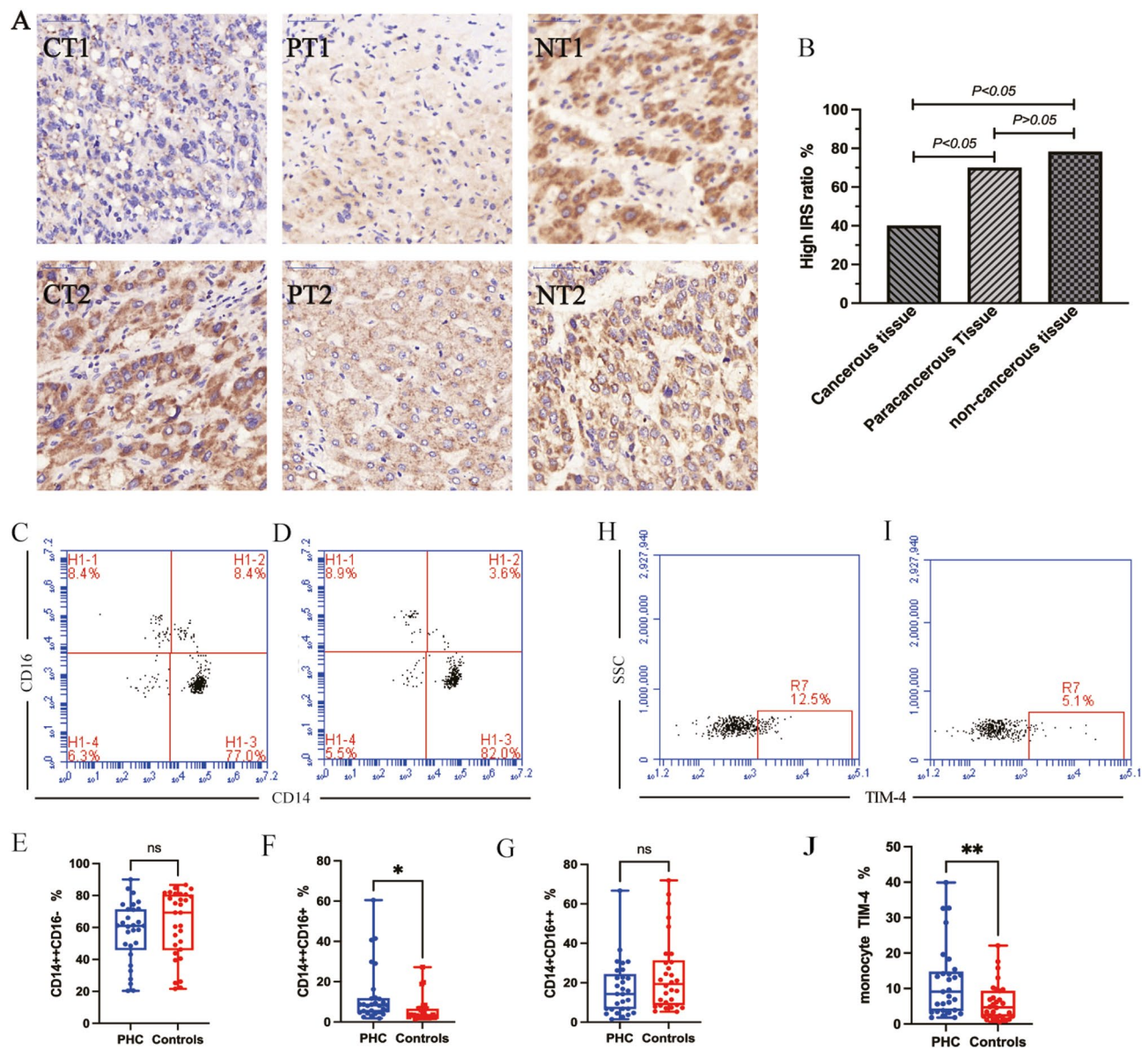


Fig. 4. (A) IHC staining ($40\times$) of TIM-4 in the liver cancer tissue (CT), paracancerous tissue (PT) and non-cancerous liver tissue (NT). CT/PT/NT1 (low expression); CT/PT/NT2 (high expression) (B) Statistical graph of TIM-4 expression level of IHC. (C) Flowchart of monocyte subsets in the PHC group; (D) Flowchart of monocyte subsets in the normal control group; (E) Statistical chart of the expression difference in classical monocyte subsets in the PHC and control groups; (F) Statistical graph of the difference in the expression of intermediate-type monocyte subsets in the PHC and control groups; (G) Statistical graph of the difference in the expression of non-classical monocyte subsets in the PHC and control groups. (H) Flowchart of the expression of TIM-4 in the monocyte subsets of PHC patients; (I) Flowchart of the expression of TIM-4 in monocyte subsets of the normal control group; (J) Flowchart of TIM-4 expression in PHC; statistical chart of the expression of total monocytes in the control group.

These results suggest that while classical monocyte levels are not significantly different, they tend to be lower in PHC patients. The significant elevation of intermediate monocytes in PHC indicates a possible phenotypic transition from classical to intermediate subsets, which may be implicated in PHC pathogenesis and progression.

Expression level of TIM-4 in blood-circulating monocytes of PHC patients

Further analysis of TIM-4 expression in monocytes and their subsets revealed that TIM-4 was expressed at significantly higher levels in PHC patients—9.1% (IQR: 3.65–14.8) compared to 4.7% (IQR: 2.05–9.4) in controls ($P < 0.05$) (Fig. 4H–J). Given the central role of monocytes in immune regulation, the elevated TIM-4 expression in circulating monocytes of PHC patients may contribute to altered immune function and tumor immune evasion.

Expression level of TIM-4 in blood-circulating monocyte subsets of PHC patients

Flow cytometry analysis revealed a significant upregulation of TIM-4 expression on circulating blood monocytes in patients with PHC. Given that monocyte subsets exhibit distinct biological functions, this study further investigated TIM-4 expression across different subsets. Monocytes were labeled with CD14 and CD16 antibodies to distinguish subsets and analyzed via flow cytometry (Fig. 5A,B). The results indicated no significant difference in TIM-4 expression within classical monocytes between the PHC and control groups ($P > 0.05$). Notably, TIM-4 was predominantly expressed in the intermediate subset (CD14 $++$ CD16 $+$). The proportion of TIM-4-positive intermediate monocytes was significantly higher in the PHC group (91.7%, IQR: 78.0–95.90) compared to the control group (73.85%, IQR: 57.7–85.3), with $P < 0.05$ (Fig. 5C). Conversely, the proportion of TIM-4-positive non-classical monocytes was significantly lower in the PHC group (6.7%, IQR: 0–14.6) compared to controls (31.1%, IQR: 2.88–38.95), $P < 0.05$ (Fig. 5D). TIM-4 positivity in classical monocytes ranged from 0 to 2.3% in the PHC group and 0–2.07% in controls, with no statistical significance ($P > 0.05$; Fig. 5E). These findings suggest that TIM-4 is primarily expressed in intermediate monocytes and is significantly elevated in PHC patients.

Correlation between the expression level of TIM-4 in blood-circulating monocytes and the commonly used clinical liver function indexes

Further flow cytometry analysis confirmed that elevated TIM-4 expression in PHC patients was predominantly confined to intermediate monocytes. This expression was correlated with AFP and several liver function biomarkers, including TBIL, ALP, GGT, ALT, AST, ALB, and PA. Specifically, TIM-4 levels showed a positive correlation with AFP, AST, GGT, and ALP, and a negative correlation with ALB and the albumin-to-globulin ratio, indicating a meaningful association. Moreover, TIM-4 expression in intermediate monocytes was negatively correlated with leukocyte ratio and PA but showed no significant correlation with AFP (Table 1). Collectively, these results suggest that TIM-4 expression may reflect both hepatocellular injury and impaired liver synthetic function.

Expression of sTIM-4 protein in peripheral blood

ELISA measurements of plasma sTIM-4 concentrations demonstrated significantly elevated levels in the PHC group [11.39 ng/mL (IQR: 6.76–18.47)] compared to the control group [5.44 ng/mL (IQR: 2.86–8.03)], with $P < 0.05$ (Fig. 5F). This finding indicates that sTIM-4 is highly expressed in the plasma of PHC patients and may be implicated in disease progression.

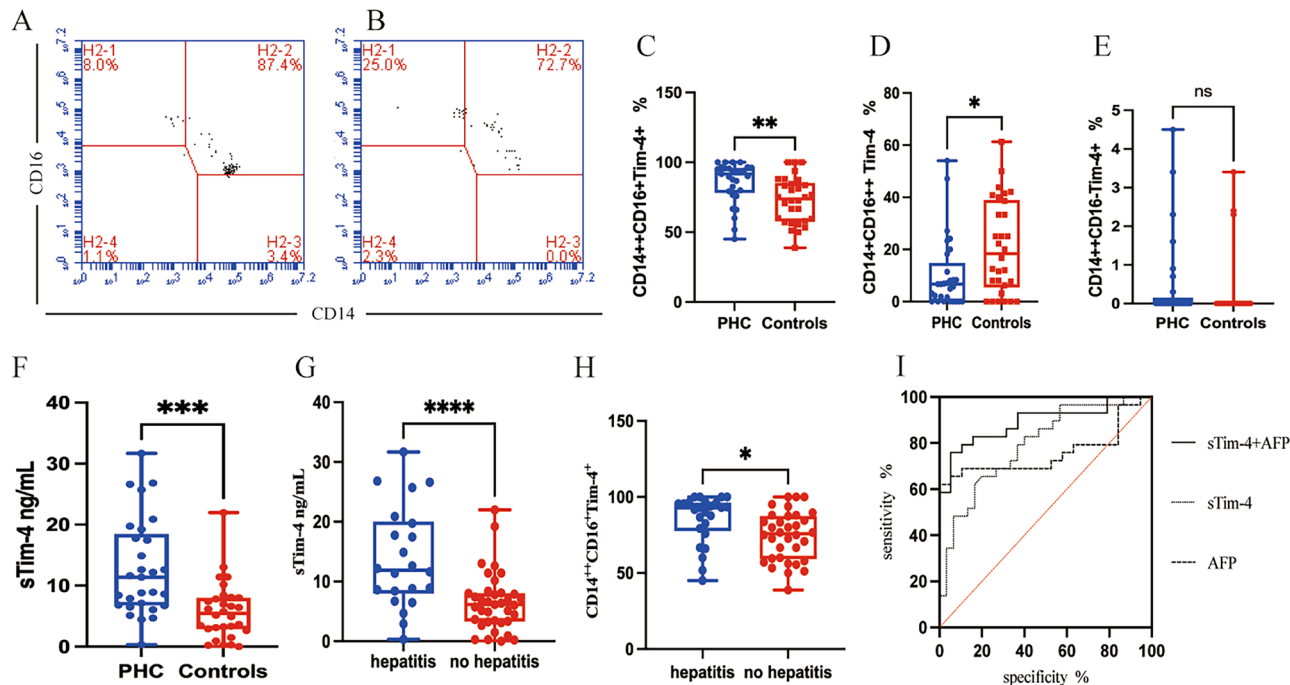


Fig. 5. (A) Flowchart of TIM-4 expression in the monocytes of PHC patients. (B) Flowchart of TIM-4 expression in the monocytes of patients in the normal control group. (C) Flowchart of TIM-4 expression in the PHC and control groups intermediate-type mononuclear cells. Statistical graph of the expression of nuclear cell subsets. (D) Statistical graph of the expression of TIM-4 in non-classical monocyte subsets in the PHC and control groups. (E) TIM-4 in classical monocytes in the PHC and control groups. Statistical chart of subpopulation expression. (F) Concentration of sTIM-4 in plasma. (G) Statistical chart of the differences in the expression levels of sTIM-4 between the hepatitis and non-hepatitis groups. (H) Intermediate-type monocyte subset Tim-4 between the hepatitis group and the non-hepatitis group. (I) ROC curve of AFP combined with sTIM-4 for the diagnosis of PHC.

	Monocyte TIM-4		CD14 ⁺⁺ CD16 ⁺ TIM-4 ⁺		sTIM-4	
	r	P	r	P	r	P
AFP	0.306	0.034*	0.281	0.053	0.322	0.026*
ALT	0.093	0.488	0.037	0.782	0.275	0.037*
AST	0.332	0.011*	0.077	0.565	0.039	0.772
GGT	0.322	0.015*	0.069	0.610	0.424	0.01*
ALP	0.294	0.027*	0.1	0.460	0.312	0.018*
ALB	-0.451	0.000***	-0.248	0.063	-0.353	0.007
A/G	-0.439	0.001**	-0.300	0.023*	-0.245	0.066
PA	-0.204	0.247	-0.399	0.019*	-0.278	0.112
TBIL	0.103	0.448	0.229	0.089	0.446	0.01*

Table 1. Correlation analysis of the expression ratio of TIM-4 in monocytes and intermediate-type monocytes and the concentration of plasma sTIM-4 with AFP and routine biochemical indexes. *P<0.05, **P<0.01, ***P<0.001.

	Sensitivity	Specificity	Youden Index	P	AUC
AFP	62.07	100	0.6207	0.0004**	0.757
sTIM-4	62.52	80	0.4552	<0.0001***	0.793
sTIM4 + AFP	75.86	94.74	0.7060	<0.0001***	0.891

Table 2. Analysis results of AFP combined with sTIM-4 to improve the diagnostic efficacy of PHC. *P<0.05, **P<0.01, ***P<0.001.

Pearson correlation analysis revealed that plasma sTIM-4 concentrations were positively correlated with AFP, ALT, ALP, GGT, and TBIL, and negatively correlated with ALB (Table 1), further supporting its relevance to liver dysfunction and tumor markers.

Correlation between the expression of TIM-4 and the history of hepatitis

Since hepatitis virus infection is a major risk factor for PHC, the PHC cohort and control group were stratified based on hepatitis history (25 with, 35 without). sTIM-4 levels were significantly higher in patients with a hepatitis history [11.62 ng/mL (IQR: 6.83–18.75)] than those without [6.10 ng/mL (IQR: 3.21–8.03)], P<0.05 (Fig. 5G). Similarly, TIM-4 expression in intermediate monocytes was elevated in the hepatitis group [92.9% (IQR: 77.6–96.35)] compared to the non-hepatitis group [75.85% (IQR: 59.18–87.55)], P<0.05 (Fig. 5H). These results suggest that the upregulation of TIM-4 may be closely associated with hepatitis virus-related liver pathology.

Diagnostic efficacy of venous blood sTIM-4 protein concentration in PHC

Our findings indicate that sTIM-4 is markedly elevated in the plasma of PHC patients and may serve as a potential diagnostic biomarker. A plasma sTIM-4 concentration ≥ 8.08 ng/mL demonstrated diagnostic utility for PHC, with an area under the ROC curve (AUC) of 0.793, a sensitivity of 62.52%, and a specificity of 80%, representing a modest improvement over AFP alone. ROC curve analysis identified diagnostic thresholds of $\text{AFP} \geq 6.93$ ng/mL and $\text{sTIM-4} \geq 8.08$ ng/mL as indicative of PHC. Notably, combining sTIM-4 with AFP significantly improved the AUC, sensitivity, and specificity, enhancing diagnostic accuracy, and the AUC difference between the two ROC curves was statistically significant ($P=0.0214 < 0.05$; Fig. 5I and Table 2).

Based on ROC curve analysis, AFP levels ≥ 6.93 ng/mL were defined as positive, and levels < 6.93 ng/mL as negative. Similarly, sTIM-4 levels ≥ 8.08 ng/mL were considered elevated, while levels < 8.08 ng/mL were regarded as normal. Univariate logistic regression analysis was conducted using patient characteristics, including hepatitis history, age (≥ 50 years defined as older, < 50 years as younger), and gender, as well as AFP and sTIM-4 levels. Variables with $P < 0.05$ in the univariate analysis were subsequently included in a multivariate logistic regression model to identify independent risk factors for primary hepatocellular carcinoma (PHC). Statistical significance was defined as $P < 0.05$. The regression analysis identified AFP positivity and a history of hepatitis virus infection as independent risk factors for PHC. Additionally, patients with elevated sTIM-4 levels had a 2.29-fold increased risk of PHC compared to those with normal sTIM-4 levels, indicating that elevated sTIM-4 is also a significant risk factor (Tables 3 and 4).

Discussion

Currently, treatment options for PHC include liver resection, liver transplantation, transarterial chemoembolization, radiation therapy, systemic therapy, and other modalities²¹. Among these, liver resection remains the most effective approach for achieving long-term survival. However, it is limited by stringent indications, and most patients are diagnosed at an advanced stage, having already missed the optimal window for surgical intervention. Even when surgery is feasible, intraoperative examination often reveals no visible tumor or

	B	SE	P	OR	95% confidence interval
AFP	3.383	1.096	0.002	29.455	3.435~252.57
sTIM-4	1.831	0.582	0.002	6.243	1.994~19.542
Gender	-0.446	0.706	0.527	0.640	0.160~2.553
Age	-0.557	0.642	0.386	0.573	0.163~2.016
History of hepatitis	3.983	0.864	0.000	53.667	9.876~291.628

Table 3. Univariate logistic regression analysis results.

	B	SE	P	OR	95% confidence interval
AFP	2.328	1.236	0.06	10.258	0.910~115.634
sTIM-4	0.83	0.89	0.351	2.293	0.401~13.124
History of hepatitis	2.436	0.962	0.11	11.428	1.734~75.340
Constant	-1.540	0.610	0.12	0.214	

Table 4. Multivariate logistic regression analysis results. In the regression model $P = 0.288 > 0.05$, the regression equation is meaningful.

thrombus in the remnant liver, while in other cases, residual malignancy is confirmed. Consequently, the overall prognosis of PHC remains poor. This underscores the emerging significance of targeted and immunotherapeutic strategies in PHC management.

Immunohistochemical analysis confirmed TIM-4 expression across liver cancer tissues, adjacent tissues, and non-cancerous tissues, with markedly lower levels observed in cancerous samples. This pattern is consistent with findings from The Cancer Genome Atlas (TCGA) and supports the potential utility of TIM-4 as a differential diagnostic marker for PHC. The behavior of TIM-4 is reminiscent of histone deacetylase 6 (HDAC6), a ubiquitously expressed protease in eukaryotic cells, which is known to promote transcription of oncogenes and suppress tumor suppressor genes, thereby exhibiting diverse and context-specific roles²² in tumorigenesis. These parallels suggest a significant role for TIM-4 in the progression of PHC.

Further analysis of TCGA data revealed correlations between TIM-4 expression and patient age, lymph node metastasis, pathological classification, and tumor stage, indicating its potential involvement in tumor development and progression. However, our experimental findings showed no significant association between TIM-4 expression in PHC tissues and variables such as age, sex, hepatitis B history, AFP level, tumor number, or tumor size. Nonetheless, we observed a slight increase in TIM-4 expression in tumors ≥ 5 cm in diameter compared to smaller tumors (< 5 cm), although this difference did not reach statistical significance, likely due to the limited sample size.

Previous studies have demonstrated that DNA sequence errors and methylation loss are major contributors to carcinogenesis²³. In our study, TIM-4 expression was found to be low in liver cancer tissues. Contrary to expectations, the methylation level of the TIM-4 promoter region was also significantly reduced in these tissues. This inverse relationship—low expression despite hypomethylation—suggests that TIM-4 regulation may involve complex, multifactorial mechanisms²⁴. For instance, chromatin remodeling or other epigenetic modifications may disrupt transcription factor binding despite low promoter methylation^{25,26}. Additionally, transcriptional repression may result from RB protein dysfunction leading to HDAC1/2-mediated deacetylation, or aberrant deacetylation by class II HDACs²⁷. Post-transcriptional regulation by specific miRNAs could also reduce TIM-4 protein levels²⁸ through mRNA degradation or translational inhibition. Moreover, tumor microenvironmental conditions such as hypoxia and acidosis may activate inhibitory pathways that further suppress TIM-4 transcription^{12,29}. Recent studies have demonstrated that among 10,844 genes showing strong mRNA–protein correlation, 18.4% exhibited promoter methylation associated exclusively with RNA expression, 3.5% exclusively with protein abundance, and only 13.9% with both RNA and protein levels³⁰. These findings underscore the nuanced and gene-specific regulatory role of DNA methylation in TIM-4 expression and its broader implications for tumorigenesis. Specifically, the low expression and methylation levels of TIM-4 in liver cancer warrant deeper investigation into its functional role in tumor development.

Immune cell infiltration is a critical factor in the pathogenesis of both malignant and non-malignant diseases. In the context of tumor biology, immune infiltration refers to the penetration of immune cells into the tumor immune microenvironment (TME), reflecting the dynamic interplay between immune surveillance and tumor progression. Genes highly expressed in the TME typically show a negative correlation with tumor purity, whereas genes predominantly expressed in tumor cells correlate positively. Consistent with this pattern, we observed a negative correlation between TIM-4 expression and tumor purity in PHC tissues, aligning with our previous finding that TIM-4 is downregulated in these tumors. Since immune dysregulation is a hallmark of cancer progression, immune infiltration serves as a key component of TME-driven carcinogenesis³¹. Immune cells modulate the TME to influence tumor apoptosis, immune evasion, and therapeutic resistance. Our analysis revealed that TIM-4 expression in PHC is positively correlated with infiltration levels of B cells, CD8⁺ T cells, CD4⁺ T cells, macrophages, neutrophils, and DCs. Moreover, CNVs in the TIM-4 gene appear to modulate the infiltration intensity of these immune subsets. Elevated immune infiltration is generally associated with improved

therapeutic response and survival, whereas reduced infiltration may reflect a tumor's capacity for immune evasion. These observations suggest that low TIM-4 expression in PHC corresponds to diminished immune infiltration, underscoring TIM-4's potential role in regulating the TME and its relevance to immunotherapeutic efficacy.

Tlymphocytes, as primary mediators of cellular immunity, exert direct effects on tumor cell cytotoxicity and regulation³². DCs possess robust antigen-presenting capabilities and play a pivotal role in initiating anti-tumor immune responses. Conversely, regulatory T cells (Tregs) facilitate immune evasion by dampening anti-tumor activity, thus promoting tumor progression³¹. Macrophage polarization³³, particularly the M1/M2 axis, is closely linked to oncogenesis. M1 macrophages are traditionally viewed as tumoricidal³⁴, whereas M2 macrophages contribute to cancer progression by fostering angiogenesis, lymphangiogenesis, immunosuppression, hypoxia, and metastasis¹⁹. In PHC tissues, TIM-4 expression was significantly positively correlated with monocytes and M2 macrophages, but negatively correlated with M0 macrophages, DCs, and Tregs. Notably, TIM-4 low-expression groups exhibited higher M0 macrophage infiltration, while monocyte infiltration was elevated in TIM-4 high-expression groups. Chemokines such as CCL2, secreted by tumor cells, may recruit peripheral monocytes to the TME, facilitating their transition from bone marrow to blood and eventually to tumor-associated macrophages³⁵. This recruitment contributes to a pro-tumorigenic microenvironment, with peripheral monocyte counts correlating with macrophage density and poor prognosis³⁶. These findings suggest that TIM-4 may regulate cellular immunity in PHC, particularly through its influence on monocyte recruitment and differentiation within the immune microenvironment.

Recent studies have demonstrated an increased expression of intermediate monocyte subsets in various tumor types, suggesting a strong association with tumorigenesis. Consistent with these findings, our study observed a similarly elevated expression of intermediate monocytes in patients with PHC. Specifically, the proportion of intermediate monocytes in the PHC group was significantly elevated by 8.3% (4.8–11.85), implying that PHC progression may involve a mechanism that facilitates the differentiation of classical monocytes into intermediate monocytes. Chronic inflammation, a key factor in PHC development, likely contributes to this shift. During inflammatory processes, intermediate monocytes secrete substantial quantities of pro-inflammatory cytokines, thereby amplifying the inflammatory response³⁷. Given that PHC often arises from persistent hepatic inflammation, the marked increase in intermediate monocyte subsets aligns with their established immunological roles.

Additionally, we found that TIM-4 expression was markedly elevated in circulating monocytes of the PHC group, increasing by 9.1%, which is 4.7% higher than in the control group. This upregulation parallels TIM-4 expression trends observed in various non-cancer inflammatory conditions¹⁸. Further stratified analysis revealed that TIM-4 expression in the intermediate monocyte subset reached 91.7%, significantly higher than the 73.85% observed in healthy controls. Although TIM-4 was also detected in non-classical monocytes, its expression was reduced in both non-classical and classical subsets in PHC patients. This distribution pattern suggests that TIM-4 expression correlates with the functional specialization of monocyte subsets. Literature reports indicate that intermediate monocytes contribute to tumor progression by secreting inflammatory mediators such as tumor necrosis factor- α and reactive oxygen species, fostering a pro-tumorigenic environment³⁷. Moreover, they facilitate tumor angiogenesis via matrix metalloproteinase-9 and vascular endothelial growth factor A¹⁶. In contrast, non-classical monocytes play roles in vascular homeostasis and anti-inflammatory responses by clearing damaged cells and secreting anti-inflammatory cytokines¹⁷. The dysregulation observed in PHC—characterized by reduced anti-inflammatory activity and enhanced pro-inflammatory signaling—supports the hypothesis that intermediate monocytes, in cooperation with TIM-4, may promote tumor progression. Correlation analyses further reinforced these findings. TIM-4 expression in monocytes showed positive correlations with serum markers of liver injury and dysfunction—AFP, AST, GGT, and ALP—and negative correlations with albumin (ALB) and leukocyte ratio. In intermediate monocytes specifically, TIM-4 was negatively correlated with leukocyte ratio and prealbumin (PA), but not with AFP. These patterns suggest that TIM-4 expression reflects hepatocellular injury and impaired synthetic function, and may serve as a biomarker for liver function assessment. Collectively, these findings indicate that TIM-4 is differentially expressed across monocyte subsets in the peripheral blood of PHC patients and may contribute to liver cancer development by disrupting monocyte homeostasis.

Hepatitis B virus (HBV) infection is a well-established risk factor for PHC. Our data revealed significantly elevated levels of soluble TIM-4 (sTIM-4) and TIM-4 expression on circulating intermediate monocytes in individuals with a history of HBV infection, suggesting a potential link between TIM-4 activity and HBV-mediated pathogenesis. Previous studies have shown that TIM-4 is upregulated in monocytes from patients with type 2 diabetes, where serum sTIM-4 positively correlates with C-reactive protein and negatively correlates with interleukin-1 β , indicating a negative regulatory role for TIM-4 in inflammasome³⁸ activity. Moreover, TIM-4 has been reported to inhibit macrophage activation via the NF- κ B signaling pathway, thereby protecting against lipopolysaccharide-induced endotoxic shock, further implicating TIM-4 in the modulation of inflammatory responses³⁹. Our findings extend these observations to liver disease, showing that both plasma sTIM-4 and TIM-4 expression in intermediate monocytes are significantly elevated in HBsAg-positive individuals. This supports the notion that TIM-4 is involved in HBV-related liver inflammation and may play a critical role in inflammation-driven hepatocarcinogenesis.

TIM-4 is a transmembrane protein, and under the proteolytic activity of a disintegrin and metalloproteinases (ADAM10 and ADAM17), its extracellular domain is cleaved to produce soluble TIM-4 (sTIM-4). Therefore, sTIM-4 concentration in peripheral blood serves as an indirect measure of TIM-4 expression in vivo. Our findings demonstrate that plasma sTIM-4 levels in PHC patients were elevated by an average of 11.62 ng/mL compared to normal controls (6.10 ng/mL). Furthermore, sTIM-4 levels showed a positive correlation with established liver function biomarkers—AFP, ALT, GGT, ALP, and TBIL—while being negatively correlated with

ALB, indicating a strong association with hepatocellular injury and impaired synthetic function. These findings align with sTIM-4 performance in other disease contexts, suggesting its potential clinical utility as a diagnostic biomarker.

Alpha-fetoprotein (AFP) is a well-established marker for PHC, as its levels rise sharply during hepatocarcinogenesis. Pearson correlation analysis in our study revealed that both TIM-4 expression in circulating monocytes and plasma sTIM-4 levels positively correlated with AFP concentrations and were significantly elevated in the PHC group, supporting the diagnostic potential of TIM-4. However, AFP has well-documented limitations: approximately 30% of PHC patients are AFP-negative, and its diagnostic cutoff remains controversial. According to the 2019 *Diagnostic and Treatment Guidelines for Primary Liver Cancer* issued by the National Health Commission of the People's Republic of China²⁰, an AFP threshold of 400 ng/mL improves diagnostic specificity, though this may exclude patients with lower AFP levels. Moreover, AFP is not specific to PHC and may also be elevated in non-malignant liver conditions, such as chronic hepatitis B, non-alcoholic fatty liver disease, and cirrhosis. It is moderately correlated with the severity of hepatic inflammation and fibrosis⁴⁰. Given these limitations, AFP must be supplemented with more sensitive and specific biomarkers. Our results indicate that sTIM-4 is a promising candidate. ROC curve analysis revealed that plasma sTIM-4 levels ≥ 8.08 ng/mL yielded high diagnostic accuracy for PHC, underscoring its potential as a complementary biomarker for early detection and diagnosis. The combined use of sTIM-4 and AFP for diagnosing primary hepatocellular carcinoma (PHC) demonstrated higher sensitivity and specificity compared to AFP alone. Furthermore, univariate and multivariate logistic regression analyses identified elevated serum TIM-4 (sTIM-4) as a significant risk factor for PHC, with patients exhibiting elevated levels facing a 2.29-fold increased risk. These findings suggest that sTIM-4, when used alongside AFP, can serve as a valuable adjunct diagnostic biomarker, enhancing the diagnostic efficiency for PHC through a non-invasive, straightforward, and clinically feasible approach.

TIM-4, a member of the TIM protein family, plays a crucial role in immune regulation. In the context of cancer, TIMD4 may modulate immune responses through its interactions with monocytic and macrophage cells⁴¹. These cells are key components of the tumor microenvironment and can exhibit a spectrum of phenotypes ranging from pro-inflammatory M1 to immunosuppressive M2 macrophages⁴². An imbalance toward M2 macrophages is often observed in HCC, contributing to an immunosuppressive environment that facilitates tumor progression⁴³. Our data revealing concurrent TIM-4 downregulation in PHC tissues and elevated TIM-4 on circulating monocytes represent interconnected components of an immunoregulatory axis. We propose a mechanistic link through CCL2/CCR2-mediated trafficking⁴⁴, whereby peripheral TIM-4⁺ monocytes infiltrate tumors and differentiate into tumor-associated macrophages (TAMs)⁴². Within the tumor microenvironment, these cells may suppress intratumoral TIM-4 expression while simultaneously driving M2 polarization via STAT6/PPAR γ -dependent reprogramming and IL-10/TGF- β secretion⁴². Concomitantly, diminished TIMD4 in tumor cells likely dampens MHC-II-mediated immunogenicity, creating a feed-forward immunosuppressive loop⁴⁵. This systemic-to-local crosstalk elucidates clinical correlations between circulating TIM-4⁺ monocytes and advanced disease stage while suggesting combinatorial therapeutic targeting could disrupt pro-tumorigenic signaling at both compartments.

Conclusion

Our findings further reveal that TIM-4 expression is downregulated in PHC tumor tissues and is closely associated with immune cell prognosis, particularly by monocytes and macrophages. Notably, elevated TIM-4 expression in circulating intermediate monocytes and its correlation with liver function markers reinforce its potential utility as a biomarker. The combined detection of sTIM-4 and AFP not only improves diagnostic accuracy but also aids in risk stratification. In future work, we'll investigate TIMD4's role in monocyte/macrophage polarization and liver cancer using co-culture assays, transcriptome sequencing, and animal models, with a focus on tumor growth, metastasis, immune regulation and targeted therapy.

Data availability

The data that support the findings of this study are available from the corresponding author upon reasonable request.

Received: 15 January 2025; Accepted: 30 July 2025

Published online: 13 August 2025

References

1. Sung, H. et al. Global Cancer Statistics 2020: GLOBOCAN estimates of incidence and mortality worldwide for 36 cancers in 185 countries. *CA Cancer J. Clin.* **71**, 209–249. <https://doi.org/10.3322/caac.21660> (2021).
2. Yang, Y. et al. Machine learning based on alcohol drinking-gut microbiota-liver axis in predicting the occurrence of early-stage hepatocellular carcinoma. *BMC Cancer* **24**, 1468. <https://doi.org/10.1186/s12885-024-13161-1> (2024).
3. Li, X. et al. The immunological and metabolic landscape in primary and metastatic liver cancer. *Nat. Rev. Cancer* **21**, 541–557. <https://doi.org/10.1038/s41568-021-00383-9> (2021).
4. Rumgay, H. et al. Global, regional and national burden of primary liver cancer by subtype. *Eur. J. Cancer* **161**, 108–118. <https://doi.org/10.1016/j.ejca.2021.11.023> (2022).
5. Vogel, A., Meyer, T., Sapisochin, G., Salem, R. & Saborowski, A. Hepatocellular carcinoma. *Lancet* **400**, 1345–1362. [https://doi.org/10.1016/S0140-6736\(22\)01200-4](https://doi.org/10.1016/S0140-6736(22)01200-4) (2022).
6. Singal, A. G., Kanwal, F. & Llovet, J. M. Global trends in hepatocellular carcinoma epidemiology: Implications for screening, prevention and therapy. *Nat. Rev. Clin. Oncol.* **20**, 864–884. <https://doi.org/10.1038/s41571-023-00825-3> (2023).
7. Greten, T. F. et al. Biomarkers for immunotherapy of hepatocellular carcinoma. *Nat. Rev. Clin. Oncol.* **20**, 780–798. <https://doi.org/10.1038/s41571-023-00816-4> (2023).
8. McIntire, J. J. et al. Identification of Tapr (an airway hyperreactivity regulatory locus) and the linked Tim gene family. *Nat. Immunol.* **2**, 1109–1116. <https://doi.org/10.1038/ni739> (2001).

9. Koohini, Z. et al. Analysis of PD-1 and Tim-3 expression on CD4(+) T cells of patients with rheumatoid arthritis; negative association with DAS28. *Clin. Rheumatol.* **37**, 2063–2071. <https://doi.org/10.1007/s10067-018-4076-4> (2018).
10. Kim, H. Y. et al. A polymorphism in TIM1 is associated with susceptibility to severe hepatitis A virus infection in humans. *J. Clin. Invest.* **121**, 1111–1118. <https://doi.org/10.1172/JCI41482> (2011).
11. Lu, X. Structure and functions of T-cell Immunoglobulin-domain and Mucin-domain Protein 3 in Cancer. *Curr. Med. Chem.* **29**, 1851–1865. <https://doi.org/10.2174/092986732866210806120904> (2022).
12. Liu, W. et al. Tim-4 in health and disease: Friend or foe?. *Front. Immunol.* **11**, 537. <https://doi.org/10.3389/fimmu.2020.00537> (2020).
13. Chen, L. et al. TIM-1 promotes proliferation and metastasis, and inhibits apoptosis, in cervical cancer through the PI3K/AKT/p53 pathway. *BMC Cancer* **22**, 370. <https://doi.org/10.1186/s12885-022-09386-7> (2022).
14. Peng, Q. Q. et al. Assessment of the expression and response of PD-1, LAG-3, and TIM-3 after neoadjuvant radiotherapy in rectal cancer. *Neoplasma* **68**, 742–750. https://doi.org/10.4149/neo_2021_20210N1341 (2021).
15. Zhang, J. et al. High HPK1(+)PD-1(+)TIM-3(+)CD8(+) T cells infiltration predicts poor prognosis to immunotherapy in NSCLC patients. *Int. Immunopharmacol.* **127**, 111363. <https://doi.org/10.1016/j.intimp.2023.111363> (2024).
16. Sidibe, A. et al. Angiogenic factor-driven inflammation promotes extravasation of human proangiogenic monocytes to tumours. *Nat. Commun.* **9**, 355. <https://doi.org/10.1038/s41467-017-02610-0> (2018).
17. Collison, J. L., Carlin, L. M., Eichmann, M., Geissmann, F. & Peakman, M. Heterogeneity in the locomotory behavior of human monocyte subsets over human vascular endothelium in vitro. *J. Immunol.* **195**, 1162–1170. <https://doi.org/10.4049/jimmunol.1401806> (2015).
18. Ye, Z. et al. Association of Tim-4 expression in monocyte subtypes with clinical course and prognosis in acute ischemic stroke patients. *Int. J. Neurosci.* **130**, 906–916. <https://doi.org/10.1080/00207454.2019.1709842> (2020).
19. Sezginer, O. & Unver, N. Dissection of pro-tumoral macrophage subtypes and immunosuppressive cells participating in M2 polarization. *Inflamm. Res.* **73**, 1411–1423. <https://doi.org/10.1007/s00011-024-01907-3> (2024).
20. National Health Commission of the People's Republic of China, B. o. M. A. *Diagnostic and Treatment Guidelines for Primary Liver Cancer. 2019 Edition.* (2019).
21. Liu, B. et al. Exploration of the role of EMC3-AS1 as a potential diagnostic and prognostic indicator in liver cancer. *Oncol. Lett.* **28**, 412. <https://doi.org/10.3892/ol.2024.14545> (2024).
22. Zeyu, Y., Xiaoxiao, Y., Sen, M., Bin, Z. & Yuming, G. Effect of HDAC6 on migration and invasion of hepatocellular carcinoma HepG2 cells and its mechanism. *J. Modern Oncol.* **27**, 4334–4340 (2019).
23. Neri, F. et al. Intragenic DNA methylation prevents spurious transcription initiation. *Nature* **543**, 72–77. <https://doi.org/10.1038/nature21373> (2017).
24. Yang, J. et al. Epigenetic regulation in the tumor microenvironment: Molecular mechanisms and therapeutic targets. *Signal Transduct. Target Ther.* **8**, 210. <https://doi.org/10.1038/s41392-023-01480-x> (2023).
25. Liu, L., Jin, G. & Zhou, X. Modeling the relationship of epigenetic modifications to transcription factor binding. *Nucleic Acids Res.* **43**, 3873–3885. <https://doi.org/10.1093/nar/gkv255> (2015).
26. Doughty, B. R. et al. Single-molecule states link transcription factor binding to gene expression. *Nature* **636**, 745–754. <https://doi.org/10.1038/s41586-024-08219-w> (2024).
27. Wade, P. A. Transcriptional control at regulatory checkpoints by histone deacetylases: Molecular connections between cancer and chromatin. *Hum. Mol. Genet.* **10**, 693–698. <https://doi.org/10.1093/hmg/10.7.693> (2001).
28. Kaikkonen, M. U., Lam, M. T. & Glass, C. K. Non-coding RNAs as regulators of gene expression and epigenetics. *Cardiovasc. Res.* **90**, 430–440. <https://doi.org/10.1093/cvr/cvr097> (2011).
29. Takano, Y. et al. Spatially resolved gene expression profiling of tumor microenvironment reveals key steps of lung adenocarcinoma development. *Nat. Commun.* **15**, 10637. <https://doi.org/10.1038/s41467-024-54671-7> (2024).
30. Liang, W. W. et al. Integrative multi-omic cancer profiling reveals DNA methylation patterns associated with therapeutic vulnerability and cell-of-origin. *Cancer Cell* **41**, 1567–1585 e1567. <https://doi.org/10.1016/j.ccr.2023.07.013> (2023).
31. Zhang, J. et al. Tumor-associated macrophages in tumor progression and the role of traditional Chinese medicine in regulating TAMs to enhance antitumor effects. *Front. Immunol.* **13**, 1026898. <https://doi.org/10.3389/fimmu.2022.1026898> (2022).
32. Lei, X. et al. Immune cells within the tumor microenvironment: Biological functions and roles in cancer immunotherapy. *Cancer Lett.* **470**, 126–133. <https://doi.org/10.1016/j.canlet.2019.11.009> (2020).
33. Li, C., Li, S., Zhang, J. & Sun, F. The increased ratio of Treg/Th2 in promoting metastasis of hepatocellular carcinoma. *Cir. Cir.* **90**, 187–192. <https://doi.org/10.24875/CIRU.21000361> (2022).
34. Mantovani, A. & Locati, M. Orchestration of macrophage polarization. *Blood* **114**, 3135–3136. <https://doi.org/10.1182/blood-2009-07-231795> (2009).
35. Mantovani, A., Bottazzi, B., Colotta, F., Sozzani, S. & Ruco, L. The origin and function of tumor-associated macrophages. *Immunol. Today* **13**, 265–270. [https://doi.org/10.1016/0167-5699\(92\)90008-U](https://doi.org/10.1016/0167-5699(92)90008-U) (1992).
36. Shibusaki, M. et al. The peripheral monocyte count is associated with the density of tumor-associated macrophages in the tumor microenvironment of colorectal cancer: A retrospective study. *BMC Cancer* **17**, 404. <https://doi.org/10.1186/s12885-017-3395-1> (2017).
37. Wong, K. L. et al. The three human monocyte subsets: Implications for health and disease. *Immunol. Res.* **53**, 41–57. <https://doi.org/10.1007/s12026-012-8297-3> (2012).
38. Zhao, P. et al. Increased T cell immunoglobulin and mucin domain containing 4 (TIM-4) is negatively correlated with serum concentrations of interleukin-1beta in type 2 diabetes. *J. Diabetes* **8**, 199–205. <https://doi.org/10.1111/1753-0407.12276> (2016).
39. Xu, L. et al. Tim-4 protects mice against lipopolysaccharide-induced endotoxic shock by suppressing the NF-κappaB signaling pathway. *Lab. Invest.* **96**, 1189–1197. <https://doi.org/10.1038/labinvest.2016.94> (2016).
40. Hanif, H. et al. Update on the applications and limitations of alpha-fetoprotein for hepatocellular carcinoma. *World J. Gastroenterol.* **28**, 216–229. <https://doi.org/10.3748/wjg.v28.i2.216> (2022).
41. Wang, Z., Chen, C., Su, Y. & Ke, N. Function and characteristics of TIM-4 in immune regulation and disease (Review). *Int. J. Mol. Med.* <https://doi.org/10.3892/ijmm.2022.5213> (2023).
42. Wang, S. et al. Targeting M2-like tumor-associated macrophages is a potential therapeutic approach to overcome antitumor drug resistance. *NPJ Precis. Oncol.* **8**, 31. <https://doi.org/10.1038/s41698-024-00522-z> (2024).
43. Li, D. et al. Biological impact and therapeutic implication of tumor-associated macrophages in hepatocellular carcinoma. *Cell Death Dis.* **15**, 498. <https://doi.org/10.1038/s41419-024-06888-z> (2024).
44. Chen, X. et al. CCL2/CCR2 regulates the tumor microenvironment in HER-2/neu-driven mammary carcinomas in mice. *PLoS ONE* **11**, e0165595. <https://doi.org/10.1371/journal.pone.0165595> (2016).
45. Fraccarollo, D., Geffers, R., Galuppo, P. & Bauersachs, J. Mineralocorticoid receptor promotes cardiac macrophage inflamming. *Basic Res. Cardiol.* **119**, 243–260. <https://doi.org/10.1007/s00395-024-01032-6> (2024).

Acknowledgements

This research was funded by Guangxi Natural Science Foundation Project (Grant No. 2024GXNSFAA010128, 2024GXNSFAA010112) and the National Natural Science Foundation of China (Grant No. 81960428).

Author contributions

The author of this paper, Yifeng Yang, was in charge of patient sample collection and statistics, as well as the analysis of immunohistochemistry, Flow cytometry and ELISA. Xingcai Chen and Dan Zeng provide experimental assistance to Yifeng Yang. Yan Wei was primarily responsible for the drafting of the manuscript and the organization of data, including the collection of research materials through databases. Professor Zhizhong Chen and Jilin Qing provided guidance on the conceptualization and writing of the paper. Yilian Zhao and Chao Ye were mainly responsible for supporting the data analysis part of the work. The other co-authors Mengru Xie and Xiaoxing Zhou also offered various forms of assistance and suggestions during the experiments.

Funding

The author(s) disclosed receipt of the following financial support for the research, authorship, and/or publication of this article: This work was supported by the Guangxi Natural Science Foundation Project (Grant No. 2024GXNSFAA010128 and 2024GXNSFAA010112) and the National Natural Science Foundation of China (Grant No. 81960428).

Declarations

Competing interests

The authors declare no competing interests.

Ethics approval

The study has been reviewed and approved by the Ethics Committee of the People's Hospital of Guangxi Zhuang Autonomous Region (IEC approval No.:KY-KJT-2023-111) and the People's Hospital of Guilin (IEC approval No.:2020-046KY). All procedures were conducted in accordance with the principles of the Declaration of Helsinki.

Additional information

Correspondence and requests for materials should be addressed to J.Q. or Z.C.

Reprints and permissions information is available at www.nature.com/reprints.

Publisher's note Springer Nature remains neutral with regard to jurisdictional claims in published maps and institutional affiliations.

Open Access This article is licensed under a Creative Commons Attribution-NonCommercial-NoDerivatives 4.0 International License, which permits any non-commercial use, sharing, distribution and reproduction in any medium or format, as long as you give appropriate credit to the original author(s) and the source, provide a link to the Creative Commons licence, and indicate if you modified the licensed material. You do not have permission under this licence to share adapted material derived from this article or parts of it. The images or other third party material in this article are included in the article's Creative Commons licence, unless indicated otherwise in a credit line to the material. If material is not included in the article's Creative Commons licence and your intended use is not permitted by statutory regulation or exceeds the permitted use, you will need to obtain permission directly from the copyright holder. To view a copy of this licence, visit <http://creativecommons.org/licenses/by-nc-nd/4.0/>.

© The Author(s) 2025